SCIENCE CHINA
Chemistry

• ARTICLES •
• SPECIAL ISSUE • In Honor of the 80th Birthday of Professor WANG Fosong

May 2012 Vol.55 No.5: 743–748
doi: 10.1007/s11426-012-4505-1

Large open-circuit voltage polymer solar cells by poly(3-hexylthiophene) with multi-adducts fullerenes

GONG Xiong[1*], YU TianZhi[1], CAO Yong[2] & HEEGER Alan J.[3]

[1]*Department of Polymer Engineering, College of Polymer Science and Polymer Engineering, The University of Akron, OH 44325-0301, USA*
[2]*State Key Laboratory of Luminescence Physics and Chemistry; South China University of Technology, Guangzhou 510641, China*
[3]*Department of Physics, University of California, Santa Barbara, USA*

Received October 5, 2011; accepted November 24, 2011; published online January 24, 2012

Polymer solar cells (PSCs) made by poly(3-hexylthiophene) (P3HT) with multi-adducts fullerenes, [6,6]-phenyl-C_{61}-butyric acid methyl ester ($PC_{61}BM$), $PC_{61}BM$-bisadduct ($bisPC_{61}BM$) and $PC_{61}BM$-trisadduct ($trisPC_{61}BM$), were reported. Electrochemistry studies indicated that $PC_{61}BM$, $bisPC_{61}BM$ and $trisPC_{61}BM$ had step-up distributional lowest unoccupied molecular orbital (LUMO) energy. PSCs made by P3HT with above $PC_{61}BM$s show a trend of enlarged open-circuit voltages, which is in good agreement with the energy difference between the LUMO of $PC_{61}BM$s and the HOMO of P3HT. On the contrary, reduced short-circuit currents (J_{sc}) were observed. The investigation of photo responsibility, dynamics analysis based on photo-induced absorption of composite films, P3HT:$PC_{61}BM$s and *n*-channel thin film field-effect transistors of $PC_{61}BM$s suggested that the short polaron lifetimes and low carrier mobilities were response for reduced J_{sc}. All these results demonstrated that it was important to develop an electron acceptor which has both high carrier mobility, and good compatibility with the electron donor conjugated polymer for approaching high performance PSCs.

fullerene derivative, large open circuit voltage, polaron lifetime, charge carrier mobility

1 Introduction

Semiconducting polymeric optoelectronic and electric devices have evolved into promising cost-effective alternatives to silicon-based devices. Bulk-heterojunction (BHJ) polymer solar cells (PSCs), based on electron-donating semiconducting polymers and electron-accepting fullerenes, are promising candidates for the realization of low-cost, printable, portable and flexible renewable energy sources [1]. In the past few years, PSCs fabricated by regioregular poly(3-hexylthiophene) (P3HT) blended with [6,6]-phenyl C_{61} butyric acid methyl ester ($PC_{61}BM$) have attracted extensive attention in research and development. Power conversion efficiencies (PCEs) of 4%–5% have been reported [2, 3]. However, a small open-circuit voltage, $V_{oc} \approx 0.60$ V, was observed from PSCs made by P3HT and PC61BM due to the small energy difference between the highest occupied molecular orbital (HOMO) energy of P3HT and the lowest unoccupied molecular orbital (LUMO) energy of $PC_{61}BM$. For the aim of enlarging the V_{oc}, $PC_{61}BM$-bisadduct ($bisPC_{61}BM$) and $PC_{61}BM$-trisadduct ($trisPC_{61}BM$) were developed [4–6]. However, the controversial PSCs performances were obtained by different groups. In order to address the PSCs performance versus multi-adducts fullerenes, $PC_{61}BM$s ($PC_{61}BM$, $bisPC_{61}BM$, and $trisPC_{61}BM$), we directed our attention towards the synthesis of [60] methanofullerene analogues with the preceding idea in mind: by developing two 1-(3-methoxycarbony)-propyl-1-phenyl-substituted [6,6]-$PC_{61}BM$, simplified as $bisPC_{61}BM$, and three 1-(3-methoxycarbony)-propyl-1-phenyl-substituted [6,6]-$PC_{61}BM$, simplified as $trisPC_{61}BM$. We further studied the performance of BHJ PSCs made by P3HT blended with these $PC_{61}BM$s ($PC_{61}BM$, $bisPC_{61}BM$ and $trisPC_{61}BM$). We

*Corresponding author (email: xgong@uakron.edu)

also analyzed the performance of the BHJ PSCs by steady state photoconductivity and time resolved photo-induced absorption, and the determination of mobilities via characterization of n-channel filed-effect transistors fabricated with $PC_{61}BM$s.

2 Experimental section

2.1 Synthesis of $PC_{61}BM$, $bisPC_{61}BM$ and $triPC_{61}BM$

Under nitrogen ambient, methy-l-4-benzoylbutyrate-p-tosyl hydrazone [7, 8] (9.0 g, 24 mmol) was dissolved in 180 mL of dry pyridine in a dried three-necked flask. Then, CH_3ONa (1.35 g, 24.96 mmol) was added and the mixture was stirred for 15 min. A solution of 8.64 g C_{60} (12 mmol) in 600 mL 1,2-dichlorobenzene was added and the resulting homogeneous reaction mixture was stirred at 65–70 °C for 38 h to give a purple-gel-suspension with foam on the top. After cooling to room temperature, the reaction mixture was transferred to a round bottom flask and concentrated to 30–50 mL via a rotary evaporator. The concentrated solution was added drop wise into a solvent mixture containing 500 mL hexane, 5 mL methanol and 5 mL acetone, with strong agitation to form precipitates. The precipitates were collected by filtration with G/F filter papers, and then washed with 25 mL of methanol three times, and 25 mL hexane once. After drying, 15 g of purple crude product was obtained. The crude product was charged into 350 mL of toluene and the resulting purple solution was heated and refluxed for 60 min, then cooled down to room temperature under stirring. This cooled toluene solution was filtered again with G/F filter papers, and concentrated to around 30 mL via a rotary evaporator. The 30 mL of concentrated residues was poured onto a silica gel column, and eluted with toluene first. Three different fractions were collected from toluene elute and were checked and distinguished by TLC. The first fraction was verified to be the un-reacted C_{60}, the second and the third fractions were verified to be one substituted [6,6]-$PC_{61}BM$, named $PC_{61}BM$-(1.9 g) and two substituted [6,6]-$PC_{61}BM$, named bisPC61BM (3.83 g), respectively. When the elute solvent was then changed from toluene to $CHCl_3$, one fraction, three substituted [6,6]-$PC_{61}BM$, named $trisPC_{61}BM$ (3.5 g), was collected. The synthetic approach to new methanofullerenes is depicted in Scheme 1.

$PC_{61}BM$: ^{1}H-NMR ($CDCl_3$) δ 7.93 (d, 2H, J = 7.5 Hz, Ar-*H*), 7.55 (t, 2H, J = 7.3 Hz, Ar-*H*), 7.48 (d, 1H, J = 7.0 Hz Ar-*H*), 3.73 (s, 3H, OCH_3), 2.91 (t, 2H, J = 8.0 Hz, PhCCH_2), 2.53 (t, 2H, J = 7.7 Hz, CH_2COO), 2.19 (t, 2 H, J = 7.7 Hz, CH_2CH$_2$COO). $bisPC_{61}BM$: LC-MS (FAB/NBA): *m*/*z* calculated for $C_{84}H_{28}O_4$ 1101.14, found: 1101, 721, 307 (100%), 391, 460. $trisPC_{61}BM$: LC-MS (FAB/NBA): *m*/*z* calculated for $C_{96}H_{42}O_6$ 1291.38, found: 1291, 720 (100%), 307, 391.

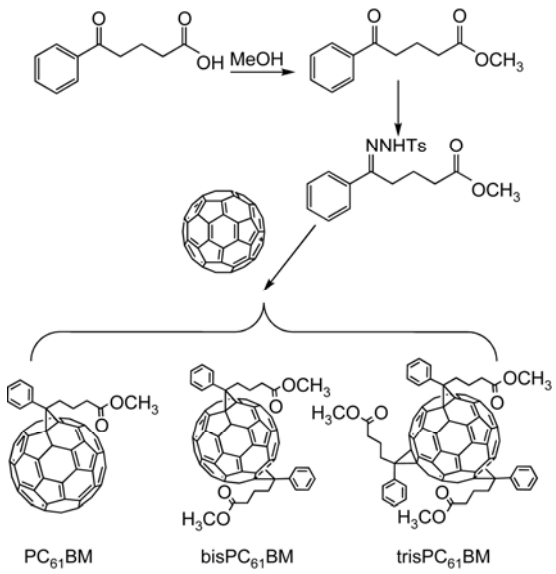

Scheme 1 Synthesis of [60] methanofullerene derivatives, $PC_{61}BM$, $bisPC_{61}BM$ and $trisPC_{61}BM$.

2.2 Cyclic voltammetry measurement

The electrochemical properties of $PC_{61}BM$, $bisPC_{61}BM$, and $trisPC_{61}BM$ were studied by cyclic voltammetry (CV) at room temperature in dichlorobenzene solution. The experiments were carried out by using tetra-*n*-butylammonium perchlorate (Bu_4NClO_4, 0.1 M) as the supporting electrolyte, a platinum as the working electrode, a platinum wire as the counter electrode, and Fc/Fc^+ as the internal reference.

2.3 BHJ PSCs

PSCs were fabricated using P3HT as the electron donor and $PC_{61}BM$ (or $bisPC_{61}BM$, or $trisPC_{61}BM$) as the electron acceptors. The ITO-coated glass substrates were cleaned subsequently by detergent, distilled water, acetone, and isopropyl alcohol in ultrasonic baths and then dried in an oven at >100 °C overnight. ~40 nm thick high conductivity PEDOT: PSS film was spin-coated (5000 r/min) from aqueous solution after treatment of the ITO substrates with UV ozone for 40 min. The substrates were dried at 160 °C for 10 min and transferred to a nitrogen-filled glovebox for spin-coating of the active layer, P3HT:$PC_{61}BM$ (or $bisPC_{61}BM$ or $trisPC_{61}BM$) layer. ~100 nm thickness of the polymer active layer, which is comprising P3HT (1.0 wt%) and $PC_{61}BM$ (or $bisPC_{61}BM$ or $trisPC_{61}BM$) (1.0 wt%) in the dichlororbenzene solution, was spin-coated on top of the PEDOT:PSS layer. Subsequently, an Al electrode (thickness ~150 nm) was thermally deposited onto the top of polymer active layer. The area of the Al electrode which defines the active area of the device was 4.5 mm^2. Current density versus voltage characterization was obtained under white light AM1.5G illumination from a calibrated solar simulator with irradiation intensity of 100 mW/cm^2.

2.4 Photoconductivity and time resolved photoinduced absorption

Films used for the photoconductivity (PC) measurement were spin-coated on alumina substrates from a 1 wt% dichlororbenzene solution, comprising P3HT (1.0 wt%) and $PC_{61}BM$ (or $bisPC_{61}BM$ or $trisPC_{61}BM$) (1.0 wt%). The thickness of the polymer layer was ~100 nm. The Auston switch sample geometry, which was with gold contacts 50 μm apart being evaporated onto the composite film, was used for PC measurement. Steady state PC measurements were carried out by the conventional modulation technique and recorded by a lock-in amplifier; the light source was a xenan lamp and the light modulation frequency was m = 170 Hz. The Xenon lamp power output and system response were characterized after each measurement with a calibrated Silicon photodiode, and then used to normalize the PC data.

Films used for time resolved photoinduced absorption (PIA) measurement were spin-coated on sapphire substrates from a 1 wt% dichlororbenzene solution, comprising P3HT (1.0 wt%) and $PC_{61}BM$ (or $bisPC_{61}BM$ or $trisPC_{61}BM$) (1.0 wt%). The thickness of the thin film is ~100 nm. The details of the experimental set-up and the measurements were given in references [9, 10].

2.5 OFET devices

n-Type organic field-effect transistors (OFETs) were fabricated on substrates which are heavily doped *n*-type Si wafers covered by a thermally grown silicon oxide (SiO_2) layer with a thickness of 200 nm. The doped Si wafer acts as a gate electrode, and the SiO_2 layer functions as a gate insulator. ~60 nm thin active layer was deposited by spin-coating from 1 wt% concentration of chloroform solution. Prior to deposition of the source and drain electrodes, the films were dried on a hot plate stabilized at 80 °C for 30 min. All fabrication processes were carried out in the glove box with nitrogen atmosphere. The source and drain electrodes, which are silver, were thermal evaporated and patterned by a shadow mask. The channel length (L) and channel width (W) were 50 μm and 2.0 mm, respectively. All OFETs were made in the top-contact geometry as shown in Figure 4(a). Electrical characterization was performed by using a Keithley semiconductor parametric analyzer (Keithley 4200) under nitrogen atmosphere. The electron mobility (μ) was determined using the following eq. (1) in the saturation regime:

$$I_{ds} = \frac{WC_i}{2L}\mu(V_{gs} - V_T)^2 = \frac{2W}{L}C_i\mu(V_{gs} - V_T)^2 \qquad (1)$$

where C_i is the capacitance per unit area of the SiO_2 dielectric (C_i = 15 nF/cm^2), I_{ds} is the drain-source current, V_{gs} is the gate-source voltage, and V_T is the threshold voltage.

3 Results and discussion

3.1 Electrochemical properties

The electrochemical properties of $PC_{61}BM$, $bisPC_{61}BM$, and $trisPC_{61}BM$ were studied by CV at room temperature in dichlorobenzene solution. The CV curves were shown in Figure 1. Table 1 summarized the data, where E^1_{red}, E^2_{red}, and E^3_{red} are the reduction potentials (defined by the onset of each reduction wave) listed together with C_{60} and $PC_{61}BM$ as references for comparison. The reduction potentials of $bisPC_{61}BM$ and $trisPC_{61}BM$ are shifted to more negative values with respect to the ones of C_{60} and $PC_{61}BM$ because of the decrease in the number of π-electrons and the release of strain energy [11, 12].

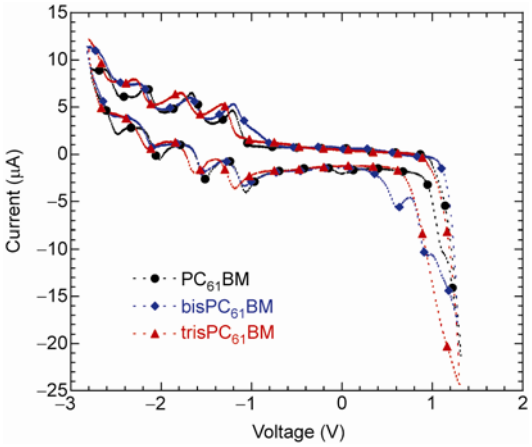

Figure 1 Cyclic voltammograms of $PC_{61}BM$, $bisPC_{61}BM$ and $trisPC_{61}BM$ in dichlorobenzene containing 0.1 M Bu_4NClO_4.

Table 1 Electrochemical data

Compound	E^1_{red}	E^2_{red}	E^3_{red}	E_{LUMO}
$PC_{61}BM$	−1.03	−1.50	−2.05	−3.77
$bisPC_{61}BM$	−1.10	−1.55	−2.11	−3.70
$trisPC_{61}BM$	−1.26	−1.65	−2.16	−3.54
$PC_{61}BM$ [11]	−1.08	−1.54	−2.04	−3.72
C_{60} [12]	−1.01	−1.46	−1.91	−3.79

In the cases of $bisPC_{61}BM$ and $trisPC_{61}BM$, the reduction values are slightly more negative than those of $PC_{61}BM$. This could be attributed to the inductive effect of the 1-(3-methoxycarbonyl)-propyl-1-phenyl group on the redox behavior. The energy levels of $PC_{61}BM$, $bisPC_{61}BM$ and $trisPC_{61}BM$ were calculated by using Ag/Ag^+ as the reference electrode, −4.65 eV, which is calibrated against the ferrocence (FOC) redox system at 4.80 eV. The reduction potentials were derived from the onset of electrochemical *n*-doping, then the LUMO energy levels were calculated according to the empirical formula: $E_{LUMO} = -(E^1_{red} + 4.65)$ (eV) [13]. The LUMO energy levels of $PC_{61}BM$, $bisPC_{61}BM$ and $trisPC_{61}BM$ are −3.77 eV, −3.70 eV and −3.54 eV, respectively. As a result, larger V_{oc} is expected to be observed from PSCs made from P3HT with either $bisPC_{61}BM$ or $trisPC_{61}BM$.

3.2 BHJ PSCs

The PCEs of PSCs are described as Eq. (2):

$$\text{PCEs} = 100(J_{sc}\times V_{oc}\times \text{FF})/P_{inc} \quad (2)$$

where V_{oc} is open-circuit voltage, J_{sc} is short-circuit current density, FF is fill factor, and P_{inc} is the intensity of incident light.

The device architecture under our investigation is a normal PSCs structure, which is ITO/PEDOT:PSS/P3HT:PC_{61}BMs/Al. The active layer was a P3HT:PC_{61}BM (or bisPC_{61}BM or trisPC_{61}BM) blend film with weight ratio of 1:1. The current density-voltage curves of PSCs are shown in Figure 2. The PSCs made by P3HT:PC_{61}BM, which serves as a standard reference for the comparison of the efficiencies with bisPC_{61}BM and trisPC_{61}BM, yielded J_{sc} of 9.56 mA/cm^2, V_{oc} of 0.55 V, FF of 0.56, resulting in PCEs of 2.94%. Under the same illumination intensity, the PSCs made by P3HT:bisPC_{61}BM exhibited J_{sc} of 7.04 mA/cm^2, V_{oc} of 0.68 V, FF of 58% and the PCEs of 2.78%. The PSCs made by P3HT:trisPC_{61}BM exhibited J_{sc} of 5.33 mA/cm^2, V_{oc} of 0.80 V, FF of 60% and the PCEs of 2.56%. The PCEs of PSCs made by P3HT:trisPC61BM decreased 16% in comparison to that of P3HT:PC_{61}BM.

V_{oc} is described as

$$V_{oc} = \frac{1}{e}(E_{\text{HOMO/Donor}} - E_{\text{LUMO/PCBM}}) - \Delta E \quad (3)$$

Where e is the elementary charge, E_{HOMO} is the HOMO energy of P3HT, E_{LUMO} is the LUMO energy of PC_{61}BMs, and ΔE is the energy difference between the build in potential and the V_{oc}, which is ascribed to the electronic loss between the electrode and active layer [14].

As expected, the V_{oc} values of both P3HT:bisPC_{61}BM and P3HT:trisPC_{61}BM are enlarged in comparison to that of P3HT:PC_{61}BM because of the lower onset reductions potential of bisPC_{61}BM and trisPC_{61}BM (Table 1). This observation is in good agreement with the energy levels of P3HT, PC_{61}BM, bisPC_{61}BM and trisPC_{61}BM, which are shown in Figure 2(b).

On the contrary, reduced J_{sc} was observed from PSCs made by P3HT:bisPC_{61}BM and P3HT:trisPC_{61}BM. Jarzab [15] suggested that the reduction of J_{sc} was a result of different microstructure of the bulk heterojunction fabricated with different acceptors. In order to address it, we have studied the steady state PC and the time resolved photo-induced absorption of the P3HT:PC_{61}BM, P3HT:bisPC_{61}BM and P3HT:trisPC_{61}BM composite films, *n*-type OFETs with PC_{61}BMs (PC_{61}BM, bisPC_{61}BM and trisPC_{61}BM) as the active layers.

3.3 Photoconductivity and time resolved photoinduced absorption

Figure 3(a) shows the steady state photoconductivity (PC) spectral profiles obtained from devices whose active layer is fabricated from blended solutions of P3HT:PC_{61}BM, P3HT:bisPC_{61}BM and P3HT:trisPC_{61}BM. The steady state PC spectral profiles of the composite films are nearly identical to their corresponding absorption spectrum. The remarkable difference is their photo responsibilities. The observed photo responsibility decreased with additional side-groups, starting from the highest photo responsibility for P3HT:PC_{61}BM, P3HT:bisPC_{61}BM, and P3HT:trisPC_{61}BM, which has the lowest photoresponsibility. The low responsibility means the absorbed photoelectrons can't be effectively used, and will be loss through radical recombination and transfer to thermal energy.

The dynamics of the photo-induced absorption (PIA) are compared in Figure 3(b). Composite thin films are pumped at 400 nm and probed at 4.5 μm. In this mid-infrared spectral region, where the polarons from the π-conjugated polymers can be detected [16]. We observed very fast decay in the P3HT: trisPC_{61}BM thin film but much longer lifetime in the P3HT:PC_{61}BM thin films. The much longer polaron lifetime (up to nanosecond) in the P3HT:PC_{61}BM composite, compared to that in the P3HT:trisPC_{61}BM thin film indicates long-lived mobile carriers, consistent with efficient charge transfer from P3HT to PC_{61}BM with inhibited back-transfer [9, 10]. The fast decay observed from the P3HT:trisPC_{61}BM composite film currently lacks a theoret-

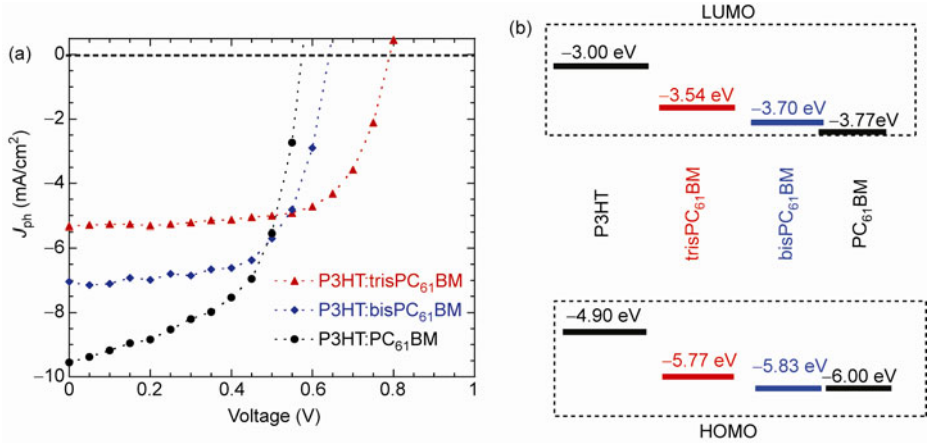

Figure 2 (a) *J-V* characteristics of polymer solar cells under AM1.5G illumination from a calibrated solar simulator with an intensity of 100 mW/cm^2; (b) schematic diagram of P3HT, PC_{61}BM, bisPC_{61}BM and trisPC_{61}BM energy levels.

ical explanation but it is probably due to the nature of trisPC$_{61}$BM. It can be morphology defects or the recombination with free electron.

3.4 *n*-Type OFETs

To explore the electron transport properties of PC$_{61}$BM, bisPC$_{61}$BM, and trisPC$_{61}$BM, field-effect mobilities were determined through the measurement of *n*-type OFETs. All n-type OFETs with the fullerenes as the active layers were fabricated on a heavily doped *n*-type Si wafer, covered by a thermally grown SiO_2 layer with a thickness of 200 nm. The OFETs geometry as shown in Figure 4(a). Ag was chosen as a metal for the source and drain electrodes to enable easy injection of electrons. A more detailed description of the fabrication process is in the Experimental Section.

Figure 4(b) shows the transport characteristics of three *n*-type OFETs fabricated with PC61BM, bisPC61BM, and trisPC61BM, respectively. All trans-conductance curves (I_{ds}-V_{gs}) are typical of good *n*-type OFETs, owing to the nature of [60] fullerene. The linear plot of $I^{1/2}$ versus V_{gs} (Figure 4(c)), deduced from the measurements of the I_{ds}

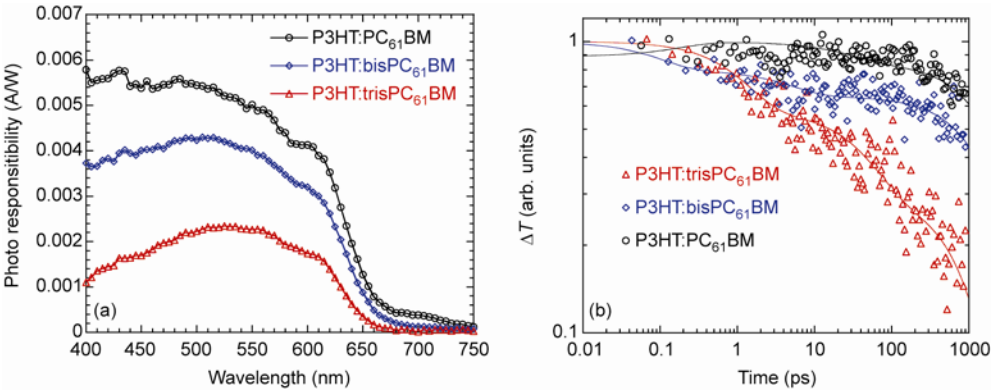

Figure 3 (a) Comparison of the steady state photoconductivities of P3HT:PC$_{61}$BM, P3HT:bisPC$_{61}$BM and P3HT:trisPC$_{61}$BM; the applied electric field for these samples was 100 kV/cm; (b) mid-IR transient decay dynamics of P3HT:PC$_{61}$BMs (PC$_{61}$BMs = PC$_{61}$BM, bisPC$_{61}$BM, or trisPC$_{61}$BM) probed at 4.5 μm.

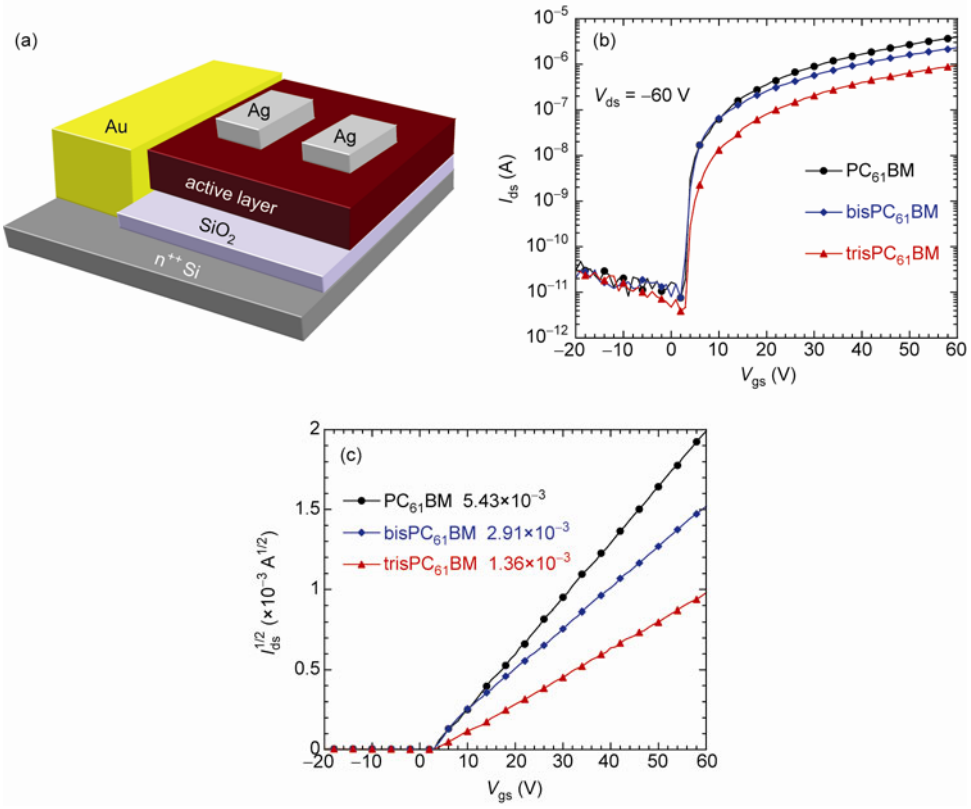

Figure 4 (a) Diagram of *n*-type OFET structure; (b) transfer characteristics of *n*-type OFETs; (c) $I^{1/2}$ vs. V_{gs} plot.

versus V_{gs}, gave electron mobilities of $\mu = 5.43\times10^{-3}$ cm^2/V s, $\mu = 2.91\times10^{-3}$ cm^2/V s, and $\mu = 1.36\times10^{-3}$ cm^2/V s for the PC61BM, bisPC61BM, and trisPC61BM, respectively. Among them, the lowest mobility value is observed in the trisPC61BM OFET. Therefore, lower mobility of trsiPC61BM is also responses for the lower performance of PSCs made by P3HT:trisPC61BM.

4 Conclusion

Mutli-adducts fullerenes, PC61BM, bisPC61BM and triPC61BM were synthesized for addressing the controversial reports from PSCs made by P3HT and mutli-adducts fullerenes. Large V_{oc} observed from PSCs made by P3HT: bisPC61BM and P3HT:triPC61BM were rational to their higher LUMO as compared with PC61BM. The investigation of the photoresponsibility, dynamics analysis of the photoinduced absorption in composite films of P3HT:PC61BMs, and *n*-channel thin film field-effect transistors of only PC61BMs suggested that the short polaron lifetimes and low carrier mobilities were response for low J_{sc}. All these results demonstrated that it was very important to develop an electron acceptor that had simultaneously both high carrier mobility, and good compatibility with the electron donor conjugated polymer for approaching high performance PSCs.

GONG X acknowledges the Joint Research Fund for Overseas Chinese Scholars, the National Natural Science Foundation of China (50828301).

1 Brabec CJ, Organic photovoltaics: Technology and market. *Sol Energy Mater Sol Cells*, 2004, 83: 273–292
2 Ma WL, Yang CY, Gong X, Lee KH, Heeger AJ. Thermally stable efficient polymer solar cells with nanoscale control of the interpenetrating network morphology. *Adv Funct Mater*, 2005, 15: 1617–1622
3 Li G, Shrotriya V, Huang JS, Yao Y, Moriarty T, mery K, Yang Y. High-efficiency solution processable polymer photovoltaic cells by self-organization of polymer blends. *Nat Mater*, 2005, 4: 864–868
4 Lenes M, Wetzlaer AH, Kooist FB, Veenstra SJ, Hummelen JC, and Blom PWM. Fullerene bisadducts for enhanced open-circuit voltages and efficiencies in polymer solar cells. *Adv Mater*, 2008, 20: 2116–2119
5 Lenes M, Shelton SW, Sieval AB, Kronholm DF, Hummelen JC, Blom PWM. Electron trapping in higher adduct fullerene-based solar cells. *Adv Func Mater*, 2009, 19: 3002–3007
6 Choi JH, Son KI, Kim T, Kim K, Ohkubo K, Fukuzumi S. Thienyl-substituted methanofullerene derivatives for organic photovoltaic cells. *J Mater Chem*, 2010, 20: 475–482
7 Keshavarz-K M, Knight B, Srdanov G, Wudl F. Cyanodihydrofullerenes and dicyanodihydrofullerene: The first polar solid based on C60. *J Am Chem Soc*, 1995, 117: 11371–11372
8 Hummelen JC, Knight BW, Wudl F, Yao J, Wilkins CL. Preparation and characterization of fulleroid and methanofullerene derivatives. *J Org Chem*, 1995, 60: 532–538
9 Sheng CX, Tong MH, Singh S, Vardeny ZV. Experimental determination of the charge/neutral branching ratio η in the photoexcitation of π-conjugated polymers by broadband ultrafast spectroscopy. *Phys Rev*, 2007, B75: 085206/1-085206/7
10 Lee CH, Yu G, Moses D, Pakbaz K, Zhang C, Sariciftci NS, Heeger AJ, Wudl F. sitization of the photoconductivity of conducting polymers by fullerene C60: Photoinduced electron transfer. *Phys Rev*, 1993, B48: 15425–15433
11 Haddon RC. Chemistry of the fullerenes: The manifestation of strain in a class of continuous aromatic molecules. *Science*, 1993, 261: 545–550
12 Lamparth I, Hirsch A. Water-soluble malonic acid derivatives of C60 with a defined three-dimensional structure. *J Chem Soc Chem Commun*, 1994, 14: 1727–1728
13 Li YF, Cao Y, Gao J, Wang DL, Yu G, Heeger AJ. Electrochemical properties of luminescent polymers and polymer light-emitting electrochemical cells. *Synth Met*, 1999, 99: 243–248
14 Scharber MC, Wuhlbacher D, Koppe M, Waldauf PC, Heeger AJ, Brabec CJ. Design rules for donors in bulk-heterojunction solar cells-towards 10% energy-conversion efficiency. *Adv Mater*, 2006, 18: 789–794
15 Lenes M, Kooistra FB, Hummelen JC, Van Severen I, Lutsen L, Vanderzande D, Cleij TJ, Blom PWM. Charge dissociation in polymer: Fullerene bulk heterojunction solar cells with enhanced permittivity. *J Appl Phys*, 2008, 104: 114517/1–114517/4
16 Jarzab D, Cordella F, Lenes M. Koolstra FB, Blom PW, Hummelen JC, Loi MA. Charge transfer dynamics in polymer-fullerene blends for efficient solar cells. *J Phys Chem B*, 2009, 113: 16513–16517
17 Guldi DM, Prato M. Excited-state properties of C60 fullerene derivatives. *Acc Chem Res*, 2000, 33: 695–703